Progress In Electromagnetics Research, Vol. 141, 17–32, 2013

AUTOMATIC DESIGN OF BROADBAND GRADIENT INDEX METAMATERIAL LENS FOR GAIN ENHANCEMENT OF CIRCULARLY POLARIZED ANTENNAS

Fan-Yi Meng[1, 3, *], Rui-Zhi Liu[1], Kuang Zhang[1], Daniel Erni[2], Qun Wu[1], Li Sun[3], and Le-Wei Li[4, 5]

[1]Department of Microwave Engineering, Harbin Institute of Technology, Harbin 150001, China

[2]Laboratory for General and Theoretical Electrical Engineering (ATE), Faculty of Engineering, University of Duisburg-Essen, CENIDE — Center for Nanointegration Duisburg-Essen, D-47048 Duisburg, Germany

[3]Department of Electrical Engineering, Harbin Institute of Technology, Harbin 150001, China

[4]Institute of Electromagnetics and School of Electronic Engineering, University of Electronic Science and Technology of China, Chengdu 611731, China

[5]School of Engineering/Department of Electrical & Computer Systems Engineering, Monash University, Sunway/Clayton, Selangor 46150/Victoria 3800, Malaysia/Australia

Abstract—A broadband gradient index (GRIN) metamaterial lens for gain enhancement of circularly polarized antennas has been automatically designed, fabricated and investigated. The GRIN metamaterial lens consists of an isotropic dielectric plate with a corresponding distribution of deep-subwavelength drill holes each with the same diameter. Such drill holes have a negligible influence on both the polarization state and the spectral response of the electromagnetic wave transmitting through the resulting GRIN metamaterial lens. Therefore, the GRIN metamaterial lens is polarization-insensitive and can efficiently transform spherical waves into planar waves over a very broad frequency range keeping the initial polarization states (e.g., linear or circular) scarcely changed. In the following we have derived analytical formulas that enable the setup of distribution rules

Received 11 May 2013, Accepted 31 May 2013, Scheduled 7 July 2013

* Corresponding author: Fan-Yi Meng (fymenghit@gmail.com).

for the drill holes on the plate. Based on these formulas, the GRIN metamaterial lens can be automatically designed and easily fabricated using circuit board engraving machines. The proposed GRIN metamaterial lens has been tested by placing it on the aperture of a circularly polarized conical horn antenna. The agreement between simulation and measurement results shows that the gain of the horn antenna has been significantly increased within the whole X-band (i.e., from 8 GHz to 12 GHz) and the largest gain enhancement reaches up to 5.7 dB. In particular, the axial ratio of the horn antenna with the GRIN metamaterial lens is less than 1.6 dB.

1. INTRODUCTION

Lens antennas have attracted extensive attention owing to their excellent directional radiation performance. The most important part in any lens antenna design lies in the proper definition of the microwave lens, where the latter provides a direct access to the performance parameters such as bandwidth, gain and efficiency.

In reality, lenses have already been proposed decades ago — namely in the 1940s — as a highly efficient measure to improve the performance of antennas. In these early stages metallic lens antennas such as metal-lens antennas and wire-grid lens antennas [1], reflector lens antennas [2], spherical antennas [3], dual lens antennas [4], as well as dielectric lens antennas [5], and substrate lens antennas [6] were successfully investigated. Virtually all of these lens designs delicately rely on non-planar structures, which are difficult to fabricate especially because of the required machining accuracy. Planar antenna lenses such as artificial dielectric lenses [7] and dipole array lenses [8] may solve the problem to some extent. However, the underlying multilayer structures of artificial dielectric lenses tend to increase the transmission losses, whereas the area of the dipole array lenses is usually much larger than the aperture of the feeding horn antenna.

As research of artificial electromagnetic materials continues, metamaterials, which were first realized by Pendry [9] and Smith [10], are applied to design novel antenna lenses such as zero-index metamaterial (ZIM) lenses and GRIN metamaterials lenses. However, for most ZIM lenses, the impedance mismatch turns out to be a vital problem [11, 12]. Even though anisotropic ZIM lenses with appropriately designed constitutive tensors can provide good impedance matching to free space [13], at present, the realized anisotropic ZIM lenses are either limited in bandwidth or extremely difficult to fabricate. In [13], a planar two-dimensional anisotropic ZIM lens has been realized to increase the gain of a Vivaldi antenna

within a considerably large bandwidth, but such ZIM lenses are barely applicable to three-dimensional antennas such as horns. GRIN lenses, however, based, e.g., on properly graded metamaterials have attracted increasing attention over recent years because they are easy to fabricate (even for optical frequencies), and offer much better impedance matching to free space compared to ZIM lenses.

The initial concept of GRIN metamaterials was actually proposed by Smith et al. [14] just before the first GRIN metamaterial lens, which possessed a negative refractive index, was realized for free-space microwave focusing by Driscoll et al. [15]. Recently, GRIN metamaterial lenses consisting of resonant metamaterials with a positive index of refraction were designed to transform cylindrical or spherical waves into planar waves, yielding antennas with an increased directivity [16–25]. In particular a highly-sophisticated broadband, dual-linear-polarized, and high-directivity lens horn antenna using GRIN metamaterials, composed of multi-layer microstrip square-ring arrays, was presented in [24]. However, there are still some open issues left in the recent studies of GRIN metamaterial lenses. On one hand, all GRIN metamaterial lenses presented so far are highly polarization sensitive. Their characteristic electromagnetic response is only supported for predefined linear polarization states. Polarization-insensitive GRIN metamaterial lenses would be highly desirable for many applications, such as, e.g., satellite communications, where it is necessary to work with circularly polarized waves. For all these cases, the implementation of GRIN metamaterial lenses requires polarization-independent design concepts.

On the other hand — similar to metamaterial cloaks — ideal GRIN metamaterial lenses rely on a continuous distribution of the (effective) refractive index that is achieved by a proper grading of the unit cells in the underlying metamaterial structure. Hence, any continuous index distribution has to be approximated by a discrete set of various metamaterial sections where each of them contains unit cells either of correspondingly altered shape or with a substantially different topology. In general, the geometric parameters of the metamaterial unit cells are obtained through extensive full-wave numerical simulation with no regard for the potential applicability of any approximate analytical synthesis methodology. In this case the design procedure of GRIN metamaterial lenses may become extremely arduous, let alone the resulting high manufacturing costs.

In response to these issues, we propose a simple and highly efficient automatic design and fabrication method for broadband polarization-insensitive GRIN metamaterial lenses. The GRIN metamaterial lens encompasses a non-resonant metamaterial layer that is represented

by an isotropic dielectric slab accordingly perforated with drill holes of deep-subwavelength dimensions, where the desired polarization insensitivity is already fostered by the non-resonant nature of the underlying metamaterial. We also derive analytical formulas describing the proper distribution rules of the drill holes mimicking the intended grading of the GRIN lens. The fabricated lens structure is then both numerically and experimentally validated by placing it on the aperture of a circularly polarized conical horn antenna.

2. AUTOMATIC DESIGN METHOD OF GRIN METAMATERIAL LENS

Unlike classical microwave lenses composed of homogeneous dielectric materials with a specific surface profile, GRIN metamaterial lenses usually encompass two parallel flat boundaries with a radially varying (effective) refractive index in between. As shown in Fig. 1, an isotropic source is placed in the focus of a GRIN metamaterial lens with the thickness of t. The choice of such idealized source is justified because we are aiming at a polarization-insensitive structure. In order to transform the spherical wave radiated from the source into a plane wave that is perpendicularly emitted from the top surface of the lens structure, every optical path from the source point to the top surface should keep the same phase delay. In this case, according to Ref. [24], the radial function $n(r)$ describing the effective refractive index of the GRIN metamaterial lens must satisfy the following expression

$$n\left(r\right) = n_0 - \frac{\sqrt{L^2 + r^2} - L}{t} \tag{1}$$

where n_0 is the refractive index of dielectric material, L the distance from phase center to the incidence plane of GRIN metamaterial lens, and r the in-plane radial variable corresponding to the radius of the displayed concentric circle with its center at the origin o.

It can be easily reasoned that the key issue for realizing a polarization-insensitive GRIN metamaterial lens is to choose (1) an isotropic background material substrate, (2) a kind of feasible polarization-insensitive (and non-resonant) metamaterial unit cell, and (3) a corresponding planar distribution of those unit cells, meaning that both latter features have to cope with the circular symmetry. In our design, the GRIN metamaterial lens is realized by a dielectric slab containing a circularly symmetric distribution of deep-subwavelength drill holes, as displayed in Fig. 2. The different unit cells are organized along concentric annuli all centered at the origin o, maintaining a uniform distribution of drill holes. These holes have the same diameter

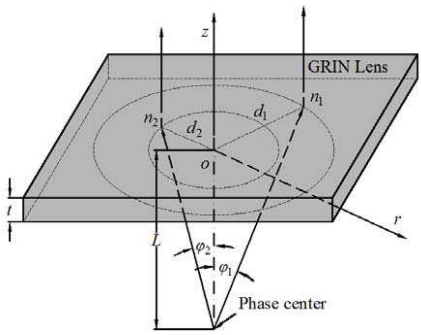

Figure 1. Geometry of the GRIN metamaterial lens.

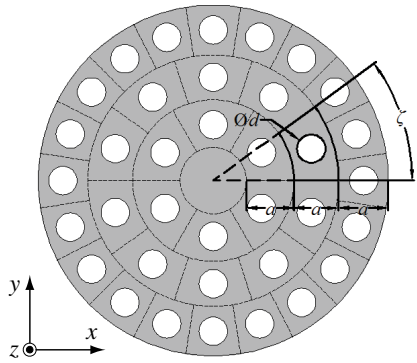

Figure 2. Top view of the GRIN metamaterial lens.

d, and are equally spaced with the same central angle ζ in the same annulus with a specific thickness a, where for different concentric annuli the central angle ζ may be different. Adopting of the dielectric plate with drill holes has presented favorable feature in designing lenses and cloaks [26–29], while the design of non-uniform drill holes restrict reducing the volume of unit cell because they need a larger area to change the radius of holes to fit the requirement of refractive index, thus it is hard to approximate the continuous distribution of gradient index in ideal situation. At the same time, the effective medium theory is fit for sub-wavelength structures, thus drill holes with large radius in the design of non-uniform drill holes would make the dielectric plate inhomogeneous. Moreover, it is much easier to control the density of holes than the radius of holes in practice. Reference [30] provides an excellent example of applying the uniform drill holes to design hemispherical lens with a constant permittivity.

To simplify the design process of the planar GRIN metamaterial lens, analytical expressions, which describe the effective refractive index as a function of the distribution of drill holes, are explored. We consider all radii of the drill holes being identical and much smaller than the operating wavelength, allowing us to use simple volume-based mixing rules to calculate effective relative permittivity of the metamaterial (respective unit cell) [31]

$$\varepsilon_{eff} = \frac{\varepsilon_d \times V_d + \varepsilon_v \times V_v}{V_d + V_v} \tag{2}$$

where $\varepsilon_{d(v)}$ and $V_{d(v)}$ are the relative permittivity and the occupied volume of the two material phases, i.e., the dielectric background and

the air hole respectively.

Based on the possibility to synthesize the metamaterial's effective refractive index we can now combine Eqs. (1) and (2) to find a distribution relation for the drill holes, which yields the graded refraction index profile for the intended spherical-to-plane-wave transformation. On the annulus with inner radius $(k-0.5)a$ and outer radius $(k+0.5)a$, the effective refractive index of the metamaterial has to match the value $n(ka)$ according to

$$\begin{cases} n\left(r\right) = n\left(ka\right) = n_0 - \dfrac{\sqrt{L^2 + \left(ka\right)^2} - L}{t} \\ r \in \left(\left(k-0.5\right)a, \left(k+0.5\right)a\right], \quad k = 1, 2, \ldots \end{cases}. \tag{3}$$

On a specific annulus, each drill hole occupies an arc-like unit cell characterized by its radial extent a and the center angle ζ as shown in Fig. 2. Referring to the mixing rule (2), the slab thickness t can be cancelled out leading to a 2D version where each volume of the metamaterial structure is represented by its corresponding footprint. Hence, the area of the unit cell A_{all} is consist of area A_d of the dielectric and area A_v of the drill hole, which leads to

$$A_d = A_{all} - A_v = \frac{2k\pi a^2 \zeta}{360} - \left(\frac{d}{2}\right)^2 \pi, \quad k = 1, 2, \ldots. \tag{4}$$

Substituting Eq. (4) into Eq. (2), the effective permittivity of the metamaterial on the annulus from $(k-0.5)a$ to $(k+0.5)a$ can be obtained as

$$\varepsilon_{\mathit{eff}} = \varepsilon_d + \frac{45d^2\left(\varepsilon_v - \varepsilon_d\right)}{ka^2\zeta}, \quad k = 1, 2, \ldots. \tag{5}$$

As the effective permeability of isotropic dielectric and air are 1, the effective refractive index $n_{\mathit{eff}} = \sqrt{\varepsilon_{\mathit{eff}}}$. By combining Eqs. (4) and (5) and the equation $n_{\mathit{eff}} = n(r)$, the central angle ζ can be derived as

$$\begin{cases} \zeta\left(r\right) = \dfrac{45d^2\left(\varepsilon_d - 1\right)}{ka^2\left(\varepsilon_d - \left(n_0 - \frac{\sqrt{L^2+(ka)^2}-L}{t}\right)^2\right)} \\ r \in \left(a\left(k-0.5\right), a\left(k+0.5\right)\right], \quad k = 1, 2, \ldots \end{cases}. \tag{6}$$

This analytical formula fully describes the distribution rule of the drill holes according to the annulus k and the associated central angle ζ, allowing the GRIN metamaterial lens to be automatically designed In another word, when the geometric parameters of horn antenna and thickness of lens are given, the formation of the lens is decided,

which means that to antennas with different parameters, we can get the construction of lens only by substituting the geometrical without reconsidering the distribution of holes.

It is worth noting that, utilizing the VBA macro programming language in the CST MW STUDIO software package, the setup of the simulation model for the designed GRIN metamaterial lens antenna can be fully automated.

3. NUMERICAL SIMULATION

In order to validate the automatic design method of the GRIN metamaterial lens, a prototype is designed based on the Eq. (6) and numerical simulations with CST Microwave Studio software package have been carried out. As shown in Fig. 3, the simulation model consists of the GRIN metamaterial lens prototype placed in the front of a conical horn antenna.

Referring to Fig. 3, the geometric dimensions of the analyzed horn antenna are chosen as $L = 101\,\text{mm}$, $d_w = 24.9\,\text{mm}$, and $R_0 = 50\,\text{mm}$. The GRIN metamaterial lens consists of a planar dielectric disk with the dimensions $R = 60\,\text{mm}$ and $t = 40\,\text{mm}$, and is made of isotropic dielectric material with a permittivity $\varepsilon_d = 2.2$. The GRIN lens is designed a little larger than the horn antenna in the radial dimension to collect potential fringing field. Referring to Fig. 2, the diameter of the drill holes amounts to $d = 0.6\,\text{mm}$ and the radial extent of the

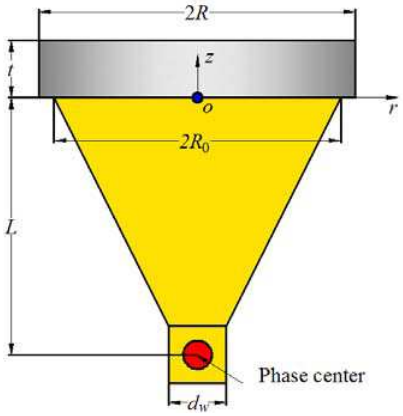

Figure 3. Sketch of the simulation model of the conical horn antenna with the GRIN metamaterial lens.

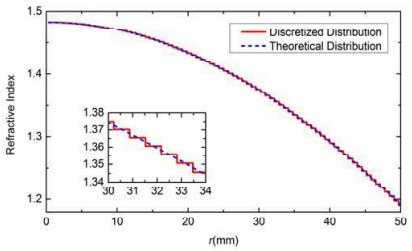

Figure 4. Comparison of the theoretical and the realized effective refractive index distribution of the GRIN metamaterial lens.

annulus is chosen to be $a = 0.65\,\text{mm}$ leading to total 92 annuli including 77 annuli positioned insider the horn antenna aperture ($r \leq 50\,\text{mm}$) and 15 annuli outside the aperture ($50\,\text{mm} < r \leq 60\,\text{mm}$). The conical horn antenna operates in the X-band from 8 GHz to 12 GHz. Substituting the above values into Eq. (6), the central angle $\zeta(r)$ of the corresponding annulus $k = 1, 2, \ldots, 77$ is calculated according to

$$\begin{cases} \zeta(r) = \dfrac{46.0118}{k\left(2.2 - \left(4.005 - \sqrt{6.3756 + 0.0264k^2}\right)^2\right)} \\ r \in (0.0065\,(k-0.5)\,, 0.0065\,(k+0.5)]\,, \quad k = 1, 2, \ldots, 77 \end{cases} \tag{7}$$

As for the distribution rule of the drill holes outside the horn antenna aperture (annulus $k = 78, 79, \ldots, 92$), we roughly design it the same as that on the annulus 77.

For visualization and comparison purposes the resulting effective refractive index profile of the GRIN metamaterial lens is calculated by Eq. (5) and $n_{eff} = \sqrt{\varepsilon_{eff}}$ using the geometric parameters above. As depicted in Fig. 4, the given theoretical index profile [cf. Eq. (1)] is accurately approximated by the discrete effective refractive index values of the synthesized GRIN metamaterial lens. And the radial extent of the annulus insures the high accuracy of approximation, which leads to better performance of beam converging.

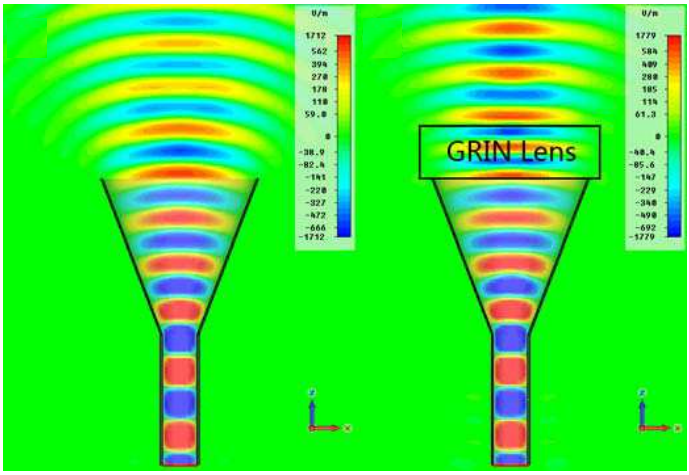

(a) (b)

Figure 5. Simulation results of the electric-field on the xoz plane of the conical horn antenna: (a) without GRIN metamaterial lens, and (b) with GRIN metamaterial lens at 10.5 GHz.

Figure 5 compares the simulated electric field distribution in the radiative near-field region of the circularly polarized conical antenna with and without the designed GRIN metamaterial lens at 10.5 GHz. In particular, Fig. 5(a) shows that the E-field distribution of the ordinary horn antenna gradually diverges; and an associated decrease in the field amplitude is observed in the radiation direction along the antenna axis. After placing the GRIN metamaterial lens in front of the horn antenna, the E-field distribution improves as expected, namely a transversally confined quasi-plane wave with virtually uniform amplitude (along the antenna axis) appears in the radiation area as shown in Fig. 5(b). All these effects are represented by a considerably reduced width of the main radiation lobe, which is tantamount to enhanced radiation directivity, and thus to an increased gain, while underpinning the intended transformation performance of the GRIN metamaterial lens.

The simulated normalized far-field radiation patterns in the *yoz* and *xoz* plane are displayed in Fig. 6 for both cases, namely the horn antenna with and without the GRIN metamaterial lens at the

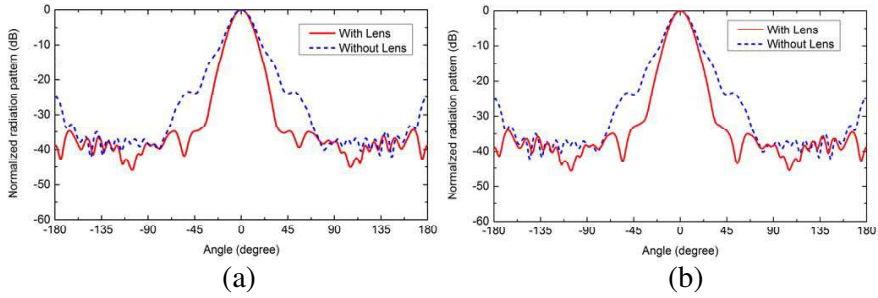

Figure 6. Simulated normalized far-field radiation patterns in the (a) *yoz* (b) *xoz* plane of the conical horn antenna with and without GRIN metamaterial lens at 10.0 GHz.

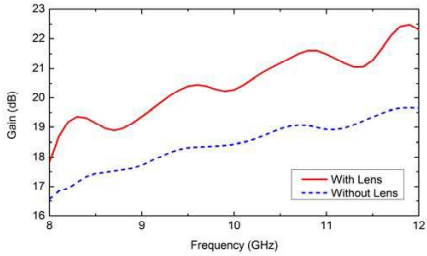

Figure 7. Simulated maximum gain spectra of the conical antenna with and without GRIN metamaterial lens.

operation frequency 10.0 GHz. From inspection one can easily deduce that the mainlobe beamwidth of the horn antenna are considerably reduced just due to the presence of the GRIN metamaterial lens.

The spectral behavior of the maximum gain is given in Fig. 7, where the simulated gain spectra of the horn antenna with and without GIRN metamaterial lens clearly indicate that the GRIN metamaterial lens can efficiently enhance the gain of the horn antenna over a very broad bandwidth ranging from 8 GHz to 12 GHz.

4. FABRICATION AND MEASUREMENT

In order to validate the electromagnetic performance of the designed GRIN metamaterial lens, a prototype sample was fabricated using a pile of seven stacked dielectric disks made of F4BMX with a permittivity $\varepsilon_d = 2.2$ and a loss tangent of 0.0007, where each of which has been identically patterned by a PCB milling machine (LPKF ProtoMat S62) and mounted them on a conical horn antenna as shown in Fig. 8. The resulting return loss is given in Fig. 9 for both cases, namely with and without the GRIN metamaterial lens. The measurements show that the broadband behavior of the horn antenna is well kept after loading the lens structure: The return loss is more than 10 dB over a frequency range of 8 GHz to 12 GHz, indicating that no additional matching layers are needed as proposed, e.g., in Ref. [25] in order to re-establish sufficient impedance matching at either air interface of the mounted metamaterial slab. To simplify the simulation, waveguide port is used to feed the antenna instead of coaxial cable, thus the pattern of simulation result differ to that of measurement, however the results share the same feature that both of them are over 10 dB in X-band.

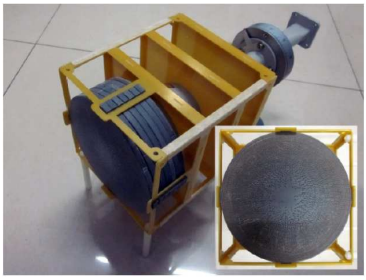

Figure 8. Prototype of the designed GRIN metamaterial lens antenna.

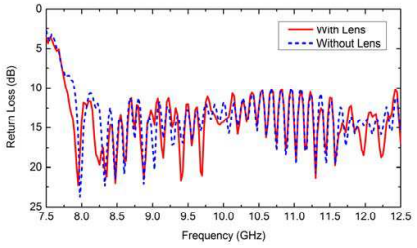

Figure 9. Measured return loss of the conical horn antenna with and without GRIN metamaterial lens.

Normalized far-field radiation patterns of the designed GRIN metamaterial lens antenna are plotted in Fig. 10 for operation frequency 10 GHz, and compared to the corresponding radiation characteristics of the unloaded horn antenna. It can be seen that, similar to the simulated results, the directivity of the horn antenna is enhanced, and the mainlobe width are decreased by the GRIN metamaterial lens. The measured gain spectrum of the designed lens antenna is compared to that of the regular horn antenna, as displayed in Fig. 11. The data reveals a gain enhancement for the lens antenna between 1.5–5.7 dB (mean value 4.3 dB) in the frequency range of 8 to 12 GHz. To simplify the simulation the feed of simulation model is the waveguide port, while coaxial cable is used to finish the measurement of the prototype. In this case, the measured results have some differences from the measured results in Fig. 7, but they both display the excellent feature of gain enhancement of the proposed lens.

Regarding now our own designed GRIN metamaterial lens we would expect a utilization factor respective aperture efficiency that is potentially increased due to the curved spreading of ray paths in the

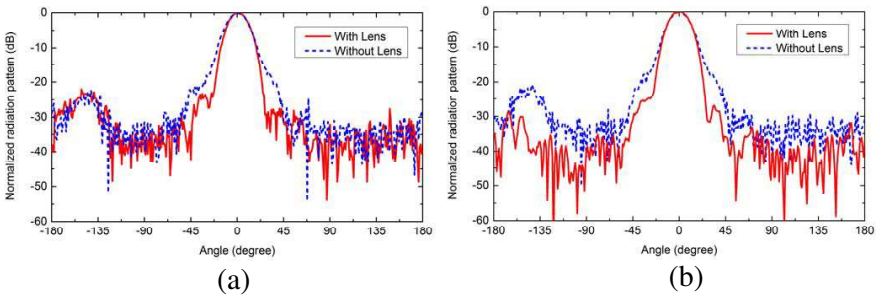

Figure 10. Measured normalized far-field radiation patterns in the (a) *yoz* (b) *xoz* plane of the circularly polarized conical horn antenna with and without GRIN metamaterial lens at 10.0 GHz.

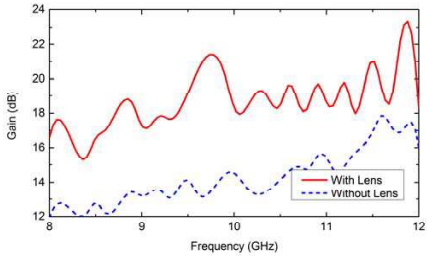

Figure 11. Measured maximum gain spectra of the circularly polarized conical antenna with and without GRIN metamaterial lens.

lens in conjunction with the cophasal wave emission at the output interface of the GRIN lens. In order to comprehensively examine the performance of the horn antenna together with the fabricated GRIN lens (cf. Fig. 8), the utilization factor of the aperture field of the horn antenna with and without the GRIN metamaterial lens are calculated from measurement data and depicted in Fig. 12. The area of horn aperture is substituted into the equation when calculating the utilization factor of horn itself while the cross-sectional area of GRIN lens on *xoy* plane is used in calculating the utilization factor of horn antenna with GRIN lens.

Given an upper bound of 0.522 [32] for the utilization factor (i.e., aperture efficiency) of the optimal circular horn antenna one easily concludes that the horn antenna in the experiment is far from optimal, but more importantly, that the designed GRIN metamaterial lens is capable to increase the utilization factor significantly — not to mention the peak values well above the upper bound. It is worth note that, in the calculation for the aperture efficiency of the GRIN lens antenna, we use the aperture dimension of the GRIN lens rather than that of the horn antenna in order to obtain convincing results.

As intended by the chosen symmetry of both, the air holes and the hole distribution the designed GRIN metamaterial lens is expected to have little impact on the polarization states of incident waves. To prove this, the axial ratio of the circularly polarized horn antenna with the GRIN metamaterial lens is analyzed and compared to the corresponding ratio of the bare feeding horn antenna. The measured axial ratio within a range of operation frequencies covering the entire X-band is shown in Fig. 13. The unloaded horn antenna emits circularly polarized radiation with an axial ratio lower than 1.5 dB in the entire operation bandwidth, whereas the inclusion of the GRIN metamaterial lens degrades the axial ratio only in the sub-range between 9.7 GHz and

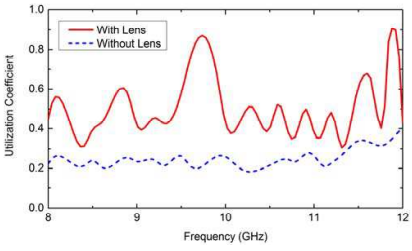

Figure 12. Measured utilization coefficient spectra for the horn antenna with and without GRIN metamaterial lens.

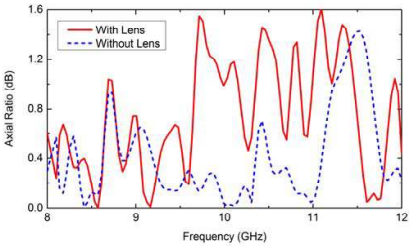

Figure 13. Measured axial ratio spectra of the circularly polarized horn antenna with and without GRIN metamaterial lens.

11.3 GHz with a maximum value below 1.6 dB. Another characteristic measure for the quality of circular polarization is the polarization efficiency as defined below

$$\eta_p = \frac{P_{co}}{P_{co} + P_{cross}} \tag{8}$$

where P_{co} and P_{cross} are the power of co-polarization and cross polarization, respectively. The resulting minimum value within the whole X-band amounts to 99.2% for the radiation field emitted after the GRIN metamaterial lens, proving a high degree of purity of the output circular polarization state.

5. CONCLUSION

This paper proposes a highly versatile automatic design method for a planar broadband GRIN metamaterial lens supporting circularly polarized waves. The underlying lens concept includes a planar dielectric disk with a tailored circular symmetric distribution of identical drilled air holes, where the density of the latter mimics the grading of the intended GRIN profile. Due to this distinct effective medium approach, and together with the maintained circular symmetry, the GRIN lens is both virtually polarization insensitive and highly broadband, while outperforming previously reported attempts based on (anisotropic) metal-dielectric GRIN metamaterials.

The excess value of the proposed design method lies in the easy-to-handle and yet highly effective analytical formalism for the calculation of the air hole distribution according to the effective grading, which realizes the intended spatial wave field transformation. The design procedure can be easily automated and linked to low cost fabrication using, e.g., a high-speed PCB milling machine providing a very flexible scheme for rapid prototyping. The thickness of lens t could be reduced by using dielectric plate with higher permittivity. In addition a GRIN lens made of F4BMX with a relative permittivity of 3.5 is simulated, and the thickness t is only 21 mm, which reduces 49% compared with the proposed lens and it also has a gain enhancement of 1 dB in average in the whole X-band.

The inherent flexibility in the overall lens manufacturing opens new possibilities for, e.g., ultra-compact mm-wave front-ends with fully integrated beam-scanning capabilities [33] providing smart user tracking in future mobile WLAN/WPAN communication and localization systems. Surprisingly, even the planar lens itself may become an attractive degree of freedom in advanced (and highly tailored) antenna system design [29] where multiple objectives are

usually at stake, for example in advanced (cognitive) MIMO systems where bandwidth, angular/spatial diversity and far-field gain are all subject to optimization.

REFERENCES

1. Kock, W. E., "Metal-lens antennas," *Proceedings of the IRE*, Vol. 34, 828–836, 1946.
2. Yaokun, Q., "Dielectric lens antenna with scan reflector," *IEEE Transactions on Aerospace and Electronic Systems*, Vol. 33, 98–101, 1997.
3. Free, W., F. Cain, C. Ryan, Jr., C. Burns, and E. Turner, "High-power constant-index lens antennas," *IEEE Transactions on Antennas and Propagation*, Vol. 22, 582–584, 1974.
4. Tang, C., "A dual lens antenna for limited electronic scanning," *IEEE Antennas and Propagation Society International Symposium*, 117–120, Urbana, IL, 1975.
5. Olver, A. D. and B. Philips, "Integrated lens with dielectric horn antenna," *Electronics Letters*, Vol. 29, 1150–1152, 1993.
6. Pavacic, A. P., D. L. del Rio, J. R. Mosig, and G. V. Eleftheriades, "Three-dimensional ray-tracing to model internal reflections in off-axis lens antennas," *IEEE Transactions on Antennas and Propagation*, Vol. 54, 604–612, 2006.
7. Abella, C., M. Marin, J. Vazquez, J. Peces, J. A. Romera, R. Graham, et al., "Artificial dielectric lens antennas: Assessment of their potential for space applications," *23rd European Microwave Conference*, 896–898, Madrid, Spain, 1993.
8. Al-Joumayly, M. A. and N. Behdad, "Wideband planar microwave lenses using sub-wavelength spatial phase shifters," *IEEE Transactions on Antennas and Propagation*, Vol. 59, 4542–4552, 2011.
9. Pendry, J. B., A. J. Holden, D. J. Robbins, and W. J. Stewart, "Magnetism from conductors and enhanced nonlinear phenomena," *IEEE Transactions on Microwave Theory and Techniques*, Vol. 47, 2075–2084, Nov. 1999.
10. Shelby, R. A., D. R. Smith, and S. Schultz, "Experimental verification of a negative index of refraction," *Science*, Vol. 292, 77–79, Apr. 2001.
11. Enoch, S., G. Tayeb, P. Sabouroux, N. Guerin, and P. Vincent, "A metamaterial for directive emission," *Physical Review Letters*, Vol. 89, 213902(4), 2002.

12. Wu, Q., P. Pan, F. Y. Meng, L. W. Li, and J. Wu, "A novel flat lens horn antenna designed based on zero refraction principle of metamaterials," *Applied Physics A — Materials Science and Processing*, Vol. 87, 151–156, 2007.
13. Zhou, B., H. Li, X. Y. Zou, and T. J. Cui, "Broadband and high-gain planar Vivaldi antennas based on inhomogeneous anisotropic zero-index metamaterials," *Progress In Electromagnetics Research*, Vol. 120, 235–247, 2011.
14. Smith, D. R., J. J. Mock, A. F. Starr, and D. Schurig, "Gradient index metamaterials," *Physical Review E*, Vol. 71, Mar. 2005.
15. Driscoll, T., D. N. Basov, A. F. Starr, P. M. Rye, S. Nemat-Nasser, D. Schurig, et al., "Free-space microwave focusing by a negative-index gradient lens," *Applied Physics Letters*, Vol. 88, 081101(3), 2006.
16. Goldflam, M. D., T. Driscoll, B. Chapler, O. Khatib, N. M. Jokerst, S. Palit, et al., "Reconfigurable gradient index using VO2 memory metamaterials," *Applied Physics Letters*, Vol. 99, 044103(3), Jul. 25, 2011.
17. Paul, O., B. Reinhard, B. Krolla, R. Beigang, and M. Rahm, "Gradient index metamaterial based on slot elements," *Applied Physics Letters*, Vol. 96, 241110(3), Jun. 14, 2010.
18. Ruopeng, L., C. Qiang, J. Y. Chin, J. J. Mock, C. Tie Jun, and D. R. Smith, "Broadband gradient index microwave quasioptical elements based on non-resonant metamaterials," *Optics Express*, Vol. 17, 21030–21041, 2009.
19. Ruopeng, L., Y. Xin Mi, J. G. Gollub, J. J. Mock, C. Tie Jun, and D. R. Smith, "Gradient index circuit by waveguided metamaterials," *Applied Physics Letters*, Vol. 94, 073506(3), Feb. 16, 2009.
20. Smith, D. R., Y.-J. Tsai, and S. Larouche, "Analysis of a gradient index metamaterial blazed diffraction grating," *IEEE Antennas and Wireless Propagation Letters*, Vol. 10, 1605–1608, 2011.
21. Yang, X. M., X. Y. Zhou, Q. Cheng, H. F. Ma, and T. J. Cui, "Diffuse reflections by randomly gradient index metamaterials," *Optics Letters*, Vol. 35, 808–810, Mar. 15, 2010.
22. Liu, Z.-G., R. Qiang, and Z.-X. Cao, "A novel broadband Fabry-Perot resonator antenna with gradient index metamaterial superstrate," *IEEE International Symposium Antennas and Propagation and CNC-USNC/URSI Radio Science Meeting*, 1–4, Toronto, 2010.
23. Lei, M. Z. and C. T. Jun, "Experimental realization of a

broadband bend structure using gradient index metamaterials," *Optics Express*, Vol. 17, 18354–18363, Sep. 28, 2009.

24. Chen, X., H. F. Ma, X. Y. Zou, W. X. Jiang, and T. J. Cui, "Three-dimensional broadband and high-directivity lens antenna made of metamaterials," *Journal of Applied Physics*, Vol. 110, 044904(8), Aug. 15, 2011.
25. Ma, H. F., X. Chen, H. S. Xu, X. M. Yang, W. X. Jiang, and T. J. Cui, "Experiments on high-performance beam-scanning antennas made of gradient-index metamaterials," *Applied Physics Letters*, Vol. 95, 094107(3), Aug. 31, 2009.
26. Mei, Z. L., J. Bai, and T. J. Cui, "Gradient index metamaterials realized by drilling hole arrays," *Journal of Physics D — Applied Physics*, Vol. 43, 055404(6), Feb. 10, 2010.
27. Ma, H. F. and T. J. Cui, "Three-dimensional broadband and broad-angle transformation-optics lens," *Nature Communications*, Vol. 1, 124(6), Nov. 2010.
28. Zhou, B., Y. Yang, H. Li, and T. J. Cui, "Beam-steering Vivaldi antenna based on partial Luneburg lens constructed with composite materials," *Journal of Applied Physics*, Vol. 110, 084908(6), 2011.
29. Ma, H. F. and T. J. Cui, "Three-dimensional broadband ground-plane cloak made of metamaterials," *Nature Communications*, Vol. 1, 21(6), 06/01/online, 2010.
30. Liu, Z. J., S. W. Yang, and Z. P. Nie, "A dielectric lens antenna design by using the effective medium theories," *International Symposium on Intelligent Signal Processing and Communication Systems (ISPACS)*, 1–4, Chendu, China, 2010.
31. Petosa, A., A. Ittipiboon, and S. Thirakoune, "Investigation on arrays of perforated dielectric fresnel lenses," *IEE Proceedings Microwaves, Antennas and Propagation*, Vol. 153, 270–276, 2006.
32. Teshirogi, T. and T. Yoneyama, *Modern Millimeter-wave Technologies*, IOS Press, Burke, VA, USA, 2001.
33. Artemenko, A., A. Mozharovskiy, A. Maltsev, R. Maslennikov, A. Sevastyanov, and V. Ssorin, "2D electronically beam steerable integrated lens antennas for mm-wave applications," *42nd European Microwave Conference (EuMC)*, 213–216, Amsterdam, the Netherlands, 2012.